ResearchGate

See discussions, stats, and author profiles for this publication at: https://www.researchgate.net/publication/231392998

Optimization and Control of Industrial Gas-Phase Ethylene Polymerization Reactors

ARTICLE *in* INDUSTRIAL & ENGINEERING CHEMISTRY RESEARCH · JUNE 1998

Impact Factor: 2.59 · DOI: 10.1021/ie980048+

CITATIONS
14

READS
41

3 AUTHORS:

Emadadeen M. Ali
King Saud University
8 PUBLICATIONS **37** CITATIONS
SEE PROFILE

A. E. Abasaeed
King Saud University
135 PUBLICATIONS **702** CITATIONS
SEE PROFILE

Saeed al-zahrani
King Saud University
138 PUBLICATIONS **1,136** CITATIONS
SEE PROFILE

Available from: Saeed al-zahrani
Retrieved on: 02 February 2016

Optimization and Control of Industrial Gas-Phase Ethylene Polymerization Reactors

E. M. Ali,* A. E. Abasaeed, and S. M. Al-Zahrani

Chemical Engineering Department, King Saud University, P.O. Box 800, Riyadh 11421, Saudi Arabia

A previously developed mathematical model for ethylene polymerization in a fluidized bed reactor was used to investigate the process static and dynamic behavior. The static analysis determined optimal operating conditions at which the monomer conversion can be increased to 25% per pass. However, this optimal operating point was shown to be unstable, and thus any changes in the plant operation may lead to temperature runaway, degrading the reactor performance. In addition, the reactor temperature must be kept within a narrow range between the gas dew point and the polymer melting point. For these reasons, two control algorithms, that is, proportional-integral (PI) and nonlinear model predictive control (NLMPC), were tested for the stabilization of the process during load changes. The PI closed-loop dynamic simulations indicated that using the reactor feed temperature solely as a manipulated variable was not sufficient to stabilize the reactor temperature. However, good PI feedback performance was obtained when the feed temperature and the superficial velocity were used to control the reactor temperature and the monomer concentration. This control structure was selected arbitrarily whereas the control structure recommended by standard methods such as RGA and SVD performed poorly. On the other hand, the NLMPC out-performed the PI control in terms of minimum tuning and controller design efforts.

1. Introduction

Control of polymerization reactors has long been known to be a difficult task. This is due to high nonlinearity of the reaction and the strong interaction of the reactor variables. For this reason there is a great deal of effort reported in the literature dealing with the control of polymerization reactors using various types of control algorithms.[1] However, there is little work on the control of gas-phase polymerization of ethylene in fluidized bed reactors. The latter has the advantage of operating at more moderate pressure and temperature than the other manufacturing processes.[2] Berber and Coskun[3] implemented quadratic dynamic matrix control (QDMC) to control the temperature of an industrial autoclave type vessel reactor for production of low-density polyethylene. Lines et al.[4] considered the real-life application of linear model predictive control to a polyethylene reactor for comprehensive control of the process. In their case product properties such as melt index and density, reactor temperature, overall conversion, production rate, and system pressure were controlled. However, their effort dealt with ethylene polymerization using a continuously stirred reactor in series with a plug flow reactor. McAuley and McGregor[5] applied a nonlinear control algorithm based on input/output linearization to the gas-phase polyethylene reaction. Their effort was devoted to minimizing the off-specs polymer during grade changeover by regulating directly the product properties. Recently, Dadebo et al.[6] examined the effect of SISO temperature control, which is based on input/output linearization, of the gas-phase polyethylene reactor. Gas-phase polyethylene reactors are prone to instability, and the reactor temperature may exhibit serious runaway.[2,6,7] The latter must be avoided, since it may lead to catalyst deactivation and serious changes in product properties. Also, most industrial gas-phase fluidized bed polyethylene reactors are operated in a narrow temperature range between 75 and 130 °C.[8] For these reasons, stabilization for polyethylene reactors is a challenging problem and needs to be addressed through good control.

Dadebo et al. demonstrated the stabilization of the polyethylene reactor temperature through a SISO control loop using the coolant temperature of an external heat exchanger as the manipulated variable.[6] This was illustrated via dynamic simulations for set point changes. Regulatory control was only demonstrated via bifurcation analysis and not through dynamic simulations. In addition, practically, the reactor feed temperature is constrained between physical bounds which in turn impose limitations on the allowable range for the coolant temperature or equivalently for the amount of heat that can be removed by the cooler. Due to this limitation, perfect regulator control over a wide range of operating conditions may not be possible.

Therefore, this work covers the effect of physical constraints imposed on the feed temperature, which in turn represent constraints on coolant temperature, on the regulatory control of the polyethylene reactor. Furthermore, improvement of the regulatory control through different control structure and/or implementation of an advanced control strategy such as nonlinear model predictive control will also be addressed. Part of this work is also to determine the optimal operating point for the reactor to provide a base case for testing the control algorithms instead of working on an arbitrary unstable operating point. Another objective of this paper is to demonstrate the advantages of using mathematical models for optimization and control design and the benefits gained from exploiting advanced control strategies for such types of processes.

* Corresponding author. E-mail address: amkamal@ksu.edu.sa. Fax: ++966-1-4678770.

S0888-5885(98)00048-7 CCC: $15.00 © 1998 American Chemical Society
Published on Web 06/26/1998

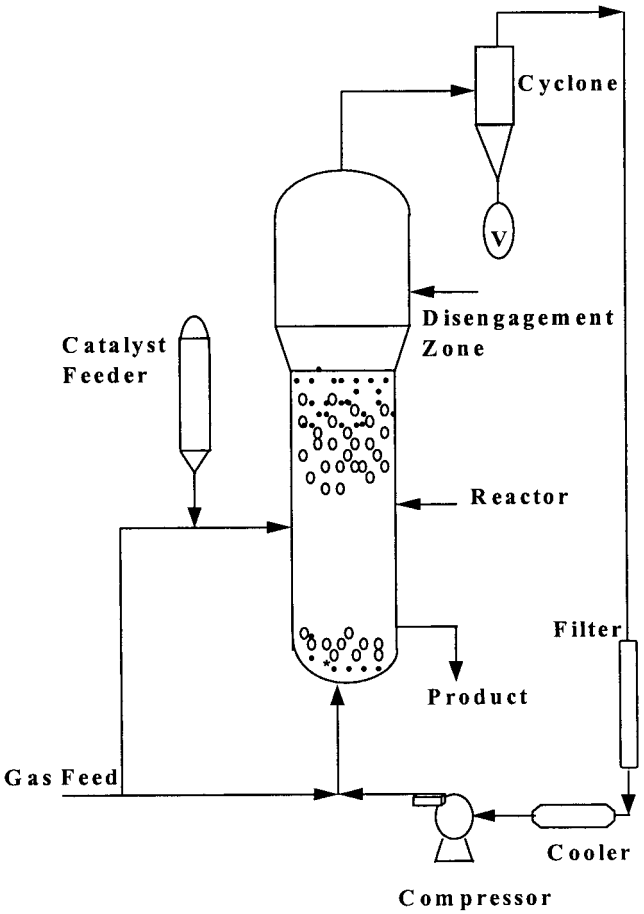

Figure 1. Schematic diagram of the fluidized bed reactor for polymerization reactions.

The paper is organized as follows; first the dynamic model of the process will be presented followed by static analysis. The static analysis consists of investigating the bifurcation behavior of the model and optimizing the process operation via optimization software. Next dynamic analysis will be performed. This includes designing the controller structure for the PI controller and formulation of the nonlinear model predictive control (NLMPC). Finally, closed-loop simulations will be presented to investigate the effectiveness of the proposed control algorithms.

2. Dynamic Model of the Reactor

Figure 1 shows a schematic diagram of a polymerization fluidized bed reactor, the UNIPOL process of Union Carbide.[9,10] The major components of the process are as follows: (a) a feed gas which is partly combined with the recycled gas before entering the bubbling fluidized bed (the other part of the fresh feed gas is used to introduce the Ziegler−Natta catalyst); (b) a catalyst feeder; (c) a product withdrawal system which is controlled in order to maintain a constant bed height inside the reactor; (d) a gas recycler which includes a cyclone and a compressor; (e) a reactor with a catalyst disengagement zone.

A simplified dynamic model is developed to describe the polymerization reaction of ethylene in a fluidized bed reactor. The model is based on the two-phase (emulsion or dense and bubble phases) theory for fluidized beds. The model assumes the following: (1) complete mixing in the emulsion phase which is at incipient fluidization and where all reactions take place; (2) that the bubble phase is devoid of solid particles and is in the plug flow regime; (3) that the bubble phase is at quasi-steady state; (4) that the catalyst injection and product withdrawal rates are adjusted in such a way that maintains a constant bed height inside the reactor; (5) that mass and heat are continuously exchanged between the bubble and emulsion phases; (6) negligible heat and mass transfer resistances between the polymer and the emulsion phase gas; (7) negligible catalyst deactivation; (8) an average bubble size at 40% of the bed height; and (9) that catalyst particles are perfect spheres. On the basis of these assumptions, the mass and energy balances resulted in the following dimensionless equations for the dense phase:

$$\frac{dX_1}{d\tau} = \alpha_3(1 - X_1) - \alpha_4(X_1 - 1)(1 - e^{-\alpha_1}) - \frac{\alpha_6 e^{-\alpha_5/X_3} X_2 X_1^{\,2}}{(X_1 + \alpha_7)} - \alpha_6 e^{-\alpha_5/X_3} X_2 X_1^{\,2} \quad (1)$$

$$\frac{dX_2}{d\tau} = \alpha_8 Q_c - \frac{\alpha_6 e^{-\alpha_5/X_3} X_2^{\,2} X_1}{(X_1 + \alpha_7)} \quad (2)$$

$$\frac{dX_3}{d\tau} = -\frac{(X_3 - 1)}{(X_1 + \gamma_1)}\frac{dX_1}{d\tau} + \frac{\gamma_5 X_1 (Y_0 - X_3)}{(X_1 + \gamma_1)} - \frac{\alpha_6 e^{-\alpha_5/X_3} X_1 X_2 (X_3 - 1)}{(X_1 + \alpha_7)} + \frac{\alpha_6 \gamma_3 e^{-\alpha_5/X_3} X_1 X_2}{(X_1 + \gamma_1)} - \frac{\gamma_4 (X_3 - Y_0)(1 - e^{-\alpha_2})}{(X_1 + \gamma_1)} - \frac{4\gamma_2 (X_3 - Y_w)}{(X_1 + \gamma_1)} \quad (3)$$

where X_1 is the dimensionless monomer concentration, X_2 is the dimensionless catalyst concentration, X_3 is the emulsion phase dimensionless temperature, Q_c is the catalyst feed rate, and τ is the dimensionless time. Detailed derivation of these equations and a description of the various parameters, that is, α_i and γ_i, and their numerical values are given elsewhere[11] and will not be repeated here.

3. Steady-State Analysis

In the following sections the steady state (static) open loop bifurcation behavior is presented.

3.1. Bifurcation Diagrams. In this preliminary investigation, the catalyst injection rate (Q_c) and the ratio between the superficial velocity and the minimum fluidization velocity ($\phi = U_0/U_{mf}$) are used as bifurcation parameters for ethylene polymerization. Note that ϕ is embedded in the model's various parameters. These two operating parameters are very important. The importance of the first parameter (catalyst injection rate) is due to the fact that the catalyst provides the nucleus upon which the polymer grows. The ratio of the velocities is important in determining the fluidization regime of the reactor, and it also affects the mass- and heat-transfer exchange parameters.

(i) Effect of Catalyst Injection Rate, Q_c. The bifurcation diagram for ethylene polymerization is shown in Figure 2 for $\phi = U_0/U_{mf} = 6$. Figure 2 relates the dimensionless ethylene concentration (X_1), and emulsion phase temperature (X_3) to the catalyst injection rate (Q_c) as the bifurcation parameter. It is clear from Figure 2a that as Q_c is increased, the ethylene

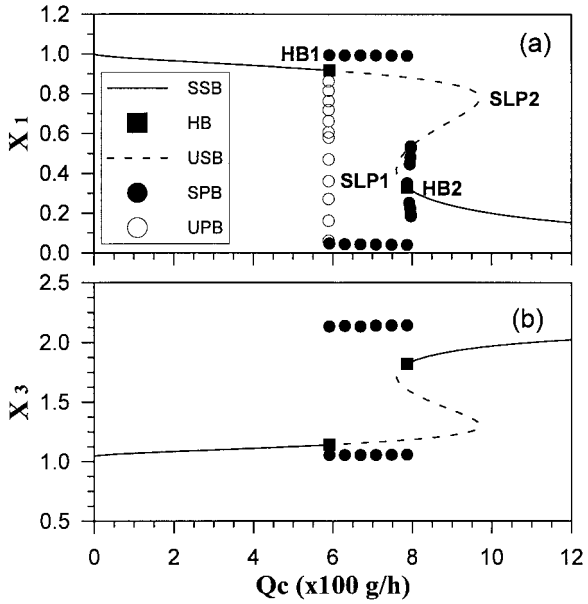

Figure 2. Bifurcation diagram for ethylene polymerization with the catalyst injection rate as the bifurcation parameter: (a) monomer concentration, X_1; (b) dense-phase temperature, X_3.

concentration decreases in a stable fashion until a Hopf bifurcation point (HB1) at $Q_c = 591.67$ g/h is reached. As Q_c is increased further, a stable periodic branch (the maxima and minima of the oscillations are denoted by ● in the figure) emanating from HB1 and which surrounds an unstable static branch (dashed lines) is the only stable attractor in the region between HB1 ($Q_c = 591.67$) and SLP1 ($Q_c = 760.42$). Operation on this oscillatory attractor is hampered by the softening temperature of polyethylene ($X_3 = 1.33$), as seen from Figure 2b, which shows that the reactor temperature reaches prohibitively high values ($X_3 > 2.0$). A multiplicity of steady states exists in the region between SLP1 and SLP2 ($Q_c = 970.69$); two unstable attractors coexist with one stable attractor. The temperature of the stable attractor which extends from HB2 ($Q_c = 787.45$) is much higher than the softening temperature of polyethylene, as shown in Figure 2b. Therefore, to operate in a stable fashion and within the safe limits of the polymer softening temperature, the polymerization reaction can only be performed at low ethylene conversion (i.e. $Q_c < 591.67$).

(ii) Effect of Gas Velocity Ratio, $\phi = U_0/U_{mf}$. Figure 3 shows the effect of the ratio of superficial velocity to minimum fluidization velocity (ϕ) on the performance of the polyethylene reactor for the catalyst feed rate $Q_c = 500$ g/h. From Figure 3, at low values of ϕ, a unique stable static branch exists with high ethylene conversion (Figure 3a) at reactor temperatures exceeding the softening temperature of the polymer (Figure 3b). The ethylene conversion decreases with increasing ϕ. Between $\phi = 2.7796$ (SLP2) and $\phi = 4.1839$ (HB1, which is a degenerate Hopf bifurcation point very close to a static limit point SLP1), three static steady-state branches coexist: two unstable branches and one stable branch still with a high reactor temperature (Figure 3b). In the region $4.2793 \leq \phi \leq 4.966$ (HB2), a stable periodic attractor surrounds an unstable static attractor. The reactor temperature obtained with the periodic attractor as it oscillates exceeds the softening temperature limits. At values of $\phi > 4.966$ a unique stable static attractor with low ethylene conversion

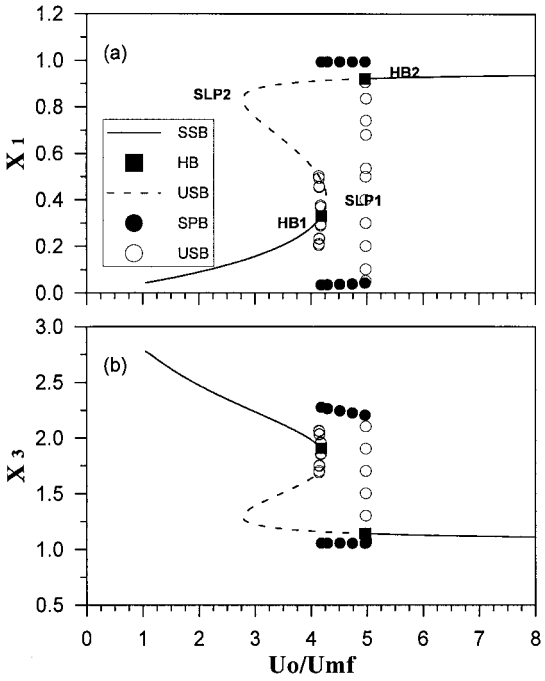

Figure 3. Bifurcation diagram for ethylene polymerization with the velocity ratio as the bifurcation parameter: (a) monomer concentration, X_1; (b) dense-phase temperature, X_3.

(Figure 3a) is present; however, the reactor temperature is well within the safe limits of softening temperature, as shown in Figure 3b.

3.2. Optimum Operating Conditions of the Reactor. Polyethylene production by gas-phase reaction suffers from low single-pass conversion (2−5%). However, according to the steady-state analysis discussed earlier and shown by Figures 2 and 3, there exists a potential for higher monomer conversion at higher catalyst feed rate (Q_c) and gas superficial velocity (U_0). However the maximum attainable conversion is limited by the softening temperature of the polymer, which is usually around 400 K (1.33 dimensionless), and by the instability of the reactor. The stability issue can be handled by proper feedback control. Thus, in this case, the optimum condition that maximizes the monomer conversion or equivalently minimizes the monomer concentration inside the reactor can be determined exactly by solving the following constrained optimization problem:

$$\min_{X_1,X_2,X_3,U_0,Q_c,T_f} z = X_1^2 \tag{4}$$

subject to

$$\frac{dX_1}{d\tau} = 0 = f_1(X_1,X_2,X_3,U_0,Q_c,T_f)$$

$$\frac{dX_2}{d\tau} = 0 = f_2(X_1,X_2,X_3,U_0,Q_c,T_f)$$

$$\frac{dX_3}{d\tau} = 0 = f_3(X_1,X_2,X_3,U_0,Q_c,T_f)$$

$$X_3 \leq 1.33$$

where T_f is the feed temperature; which is represented in eq 3 by the dimensionless variable Y_0. U_0 does not

Table 1. Optimum Operating Conditions of the Reactor

ϕ	Q_c	T_f	X_1	X_2	X_3
6.001	969.5	330	0.7524	1.202×10^{-4}	1.33

appear explicitly in these equations; however, it is lumped in the model's various parameters. It should be noted that, while carrying out the above optimization, all other reactor parameters and operating conditions are fixed. The wall temperature is assumed to be constant at its nominal value of 340 K. Similarly, the reactor total pressure and the bed height are assumed to be constant. In reality, changing U_0 and Q_c would affect the total pressure and the bed height. However, these variables are fixed through feedback control loops, which is a common practice for industrial polyethylene reactors. In fact, total pressure is controlled by manipulating the bleed stream, which is not modeled for this case but will be assumed effective, whereas the bed height is controlled by the product withdrawal, which has been accounted for in the present model. In general, a more realistic optimization of the process would include cost analysis. However, polyethylene production by a gas-phase reaction is known to have low operational cost. Hence, the objective here is rather to define the optimum operating condition considering that any increase in the operational cost is within the plant acceptable capacity. Alternatively, the cost effect can be measured, as will be shown later, by expressing the process yield as a ratio of the increase in PE productivity to the increase in catalyst usage.

Solving the above optimization problem for the given model using MATLAB results in the optimum conditions listed in Table 1. This point corresponds to a 25% conversion and will be used as the desired set point around which the control algorithms will be tested. Moreover, this point corresponds also, as demonstrated by Figures 2 and 3, to an unstable steady-state point, which makes the control problem even more challenging. It is more interesting to demonstrate the effect of various values of ϕ (i.e., U_0) and T_f on the monomer conversion, as depicted by Figure 4a−c. The plots are obtained by solving the above optimization problem for different values of U_0 and T_f using only X_1, X_2, X_3, and Q_c as the optimization parameters. In these figures, the polyethylene productivity (pp), since it is more informative, is shown instead of conversion. The former is related to the conversion as follows:

$$\mathrm{pp} = C_0(U_{mf}A(1 - X_1) + U_bA_b(X_1 - (X_1 - 1)e^{-\alpha_1}) \quad (5)$$

where C_o is the inlet monomer concentration, U_{mf} is the minimum fluidization velocity, U_b is the bubble velocity, A is the cross-sectional area of the reactor, and A_b is the area of the bubble phase.

In the objective function (eq 4) the monomer concentration is minimized instead of maximizing the PE productivity to ensure that the increase in yield is actually due to higher conversion and not due to other reasons such as higher flow rates. Figure 4a demonstrates that PE productivity and hence conversion increase monotonically with ϕ; however, higher catalyst feed rates (Q_c) are required, as shown in Figure 4b. The feed temperature (T_f) has a negligible effect on PE productivity (Figure 4a) and minimally affects Q_c (Figure 4b). The fact that conversion increases with ϕ (U_0) at the expense of Q_c reflects the need for more active sites of the catalyst. Therefore, if no upper bound was

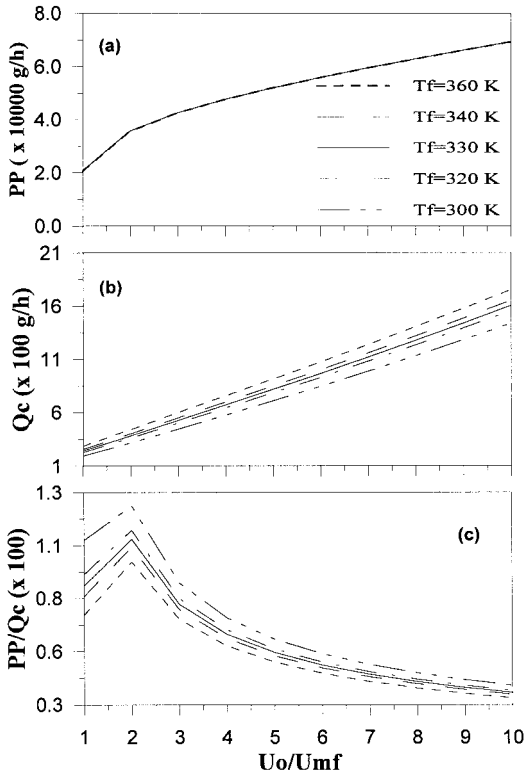

Figure 4. Optimum conditions; (a) ethylene productivity; (b) catalyst injection rate; (c) ratio of ethylene productivity to catalyst injection rate.

imposed on X_3, the maximum PE productivity would occur at the highest possible values of ϕ and Q_c. Since the maximum allowable value of Q_c is 1000 g/h (Table 1), then, as shown by Figure 4a and b, the optimum condition corresponds to $\phi = 6$, which is the same result obtained earlier. An interesting result is obtained when the PE yield is expressed as a ratio to catalyst feed rate, as illustrated by Figure 4c. In this figure, the optimum condition at $\phi = 1$ is taken as a basis, and the remaining points are related to that point. It is clear that the maximum yield per catalyst used occurs at $\phi = 2$ and that the lower feed temperature has a higher monomer conversion ratio. The latter is because the lower feed temperature requires a lower catalyst feed rate for the same monomer conversion, as indicated by Figure 4b. Usually when the catalyst is developed on site, its cost will be small relative to the price of the product. Thereby, we can still consider the operating point given in Table 1 as the optimum condition.

4. Dynamic Simulation and Control

In this section the dynamic simulation results for the open loop as well as the closed loop (using PI and NLMPC) are presented.

4.1. Polyethylene Reactor Control Objective and Design. Basically industrial PE reactors possess several control objectives. The bed height is maintained at the desired value by manipulating the product flow rate. The reactor total pressure is perfectly controlled via a bleed stream. The reactor feed temperature is usually controlled by manipulating the cooling water flow rate of an upstream heat exchanger which is used mainly to remove the heat produced by the exothermic reaction. The product quality is achieved through maintaining the ratio of the gases' partial pressures

Table 2. Manipulated Variable Constraints

variable	upper value	lower value
Q_c	10.6 ($\times 10^2$ g/h)	1 ($\times 10^2$ g/h)
ϕ	10	2
T_f	300 (K)	360 (K)

within desired targets. The latter is achieved by manipulating the gases' fresh feeds. If reliable measurements of the product properties are available, they can also be used to minimize the off-specs products during grade transition. Here we are concerned with controlling the monomer concentration and the reactor temperature that correspond to the maximum yield, assuming all other basic control loops are taken care of by other means. The importance of our proposed control objective stems from the fact that the desired optimum set point is unstable, and thus any disturbances may make the process variables drift away from the desired point. In addition, tight control of the reactor temperature is required to keep it above the dew point of the gases and below the softening temperature of the polymer.

The available manipulated variables for this case are the catalyst feed rate (Q_c), the ratio of superficial velocity to minimum fluidization velocity (ϕ), and the set point of the feed temperature (T_f). Physical constraints are imposed on these variables as listed in Table 2. The common disturbances to the process are the wall temperature, the feed temperature or coolant temperature, the inert gases' concentrations, and the catalyst feed rate. Practically, disturbances in Q_c occur due to malfunctioning of the catalyst feeder, which is very common for such processes.

For brevity, we will consider the objective of rejecting the influence of disturbances in the reactor wall temperature by means of PI and NLMPC algorithms. Also we will consider the objective of set point changes using only the NLMPC algorithm. In all the simulations hereafter, the constraints in Table 2 will always be imposed and a sampling time of 0.001 (dimensionless) is used. It should also be noted that all variables shown in the figures, including time, are dimensionless. It is worth mentioning that the PI settings are determined by the Ziegler and Nichols method.[12]

4.2. PI Control Structure Design. When a PI controller is implemented for a nonsquare multi-input multi-output (MIMO) system, the best control structure should be determined first, followed by determining the best control pairing. The best structure is the square subsystem, which is expected to have the best closed-loop performance among all the other sets of square subsystems. There are many approaches reported in the literature that deal with this situation, among which is the nonsquare relative gain array (NRGA) method,[13] which can be calculated as follows:

$$\Lambda = G \otimes (G^{+})^{T} \tag{6}$$

where G is the steady-state gain matrix of the linearized model, G^+ is the pseudoinverse of G, and $\otimes$ is defined as the element-by-element product. Cao and Rossiter[14] utilized this tool for input selection. Their input selection criteria are based on the sum of Λ columns. The ith input is considered effective if the sum of the ith column is large and vice versa. Cao and Biss[15] used another method to select the control structure. They divided the nonsquare steady gain matrix into a set of square subsystems and computed the singular value decomposition (SVD) for each set. The set with the largest SVD is taken as the most effective set. These two methods will be used here to select the best two manipulated variables for our control problem. Then the relative gain approach (RGA) will be used to obtain the best input−output pairing.[16]

Table 3. Steady-State Gains between Manipulated and Controlled Variables

	Q_c	ϕ	T_f
X_1	0.2412	−0.3781	0.009
X_3	−0.2795	0.4227	−0.0099

Table 4. Nonsquare Relative Gains between Manipulated and Controlled Variables

	Q_c	ϕ	T_f
X_1	−27.3178	28.2896	0.0282
X_3	28.3177	−27.2904	−0.0273

Table 5. Singular Value Decomposition of the Three Candidate Control Structures

control structure	σ_1	σ_2
S1	0.6766	0.0055
S2	0.5672	0.0001
S3	0.3694	0.0003

First, the nonlinear model is linearized around the optimal operating point from which the steady-state gain matrix (G) is obtained as listed in Table 3. By inspecting G, we notice that T_f has very small gains, which indicates that large changes in T_f are required to make significant effects on the controlled outputs. In this case T_f may saturate quickly and thus degrade the feedback performance. Also we notice that Q_c has the same magnitude effect on both outputs but in the opposite direction. Similarly, ϕ has almost the same magnitude effect on both outputs but in the opposite direction and in the opposite direction to the effect of Q_c. This indicates the strong interaction between these two inputs and the corresponding outputs. The above-observed phenomena will impose a challenging control problem for the PI algorithm, since it operates in a decentralized mode.

The elements of NRGA for the static gain matrix (G) are shown in Table 4. It is obvious from the sum of the columns that the third column has the smallest magnitude. Thus T_f should be eliminated from the acceptable inputs set. To use the SVD method the 2×3 system is divided into three 2×2 subsystems. We denote the first subsystem as S1 which has Q_c and ϕ as the manipulated variables (MVs), the second subsystem as S2, which has ϕ and T_f as the MVs, and the third subsystem as S3, which has Q_c and T_f as the MVs. Table 5 lists the SVD values of the three subsystems. It is clear that the S1 structure has the largest SVD; thus, it should provide the best closed-loop performance. This also coincides with the results obtained by the NRGA method. Cao and Biss[15] have extended the SVD method to consider the constrained inputs for the control structure selection. Without getting involved in the details of the proposed new method, we have tested this approach for our design problem, and the same conclusion, that is that S1 has the best structure, was also obtained. Next, the RGA for each control structure is computed and listed in Table 6. The RGA indicates highly interacting multivariable system, and thus, decentralized control such as PI will face difficulties in maintaining good reactor performance. Nevertheless, for the S1 subsystem and according to its RGA, X_1

Table 6. Relative Gains between Manipulated and Controlled Variables for Each Control Structure

	S_1		S_2		S_3	
	Q_c	ϕ	ϕ	T_f	Q_c	T_f
X_1	−27.3243	28.3243	−117.5606	118.5606	−22.0191	23.0191
X_3	28.3243	−27.3243	118.5606	−117.5606	23.0191	−22.0191

(monomer concentration) should be controlled by ϕ and X_3 (reactor temperature) by Q_c.

4.3. Nonlinear MPC Algorithm. In this paper the structure of the MPC version developed by Ali and Zafiriou[17] that utilizes directly the nonlinear model for output prediction is used. A usual MPC formulation solves the following on-line optimization:

$$\min_{\Delta u(t_k),\ldots,\Delta u(t_{k+M-1})} \sum_{i=1}^{P} ||\Gamma(y(t_k+i) - r(t_k+i)||^2 + \sum_{i=1}^{P} ||\Lambda u(t_k+i-1)||^2 \quad (7)$$

subject to

$$B^T \Delta U(t_k) \le b \quad (8)$$

For nonlinear MPC the predicted output y over the prediction horizon P is obtained by the numerical integration of

$$\frac{dx}{dt} = f(x,u,t) \quad (9)$$

$$y = g(x) \quad (10)$$

from t_k up to t_{k+P}, where x and y represent the states and the output of the model, respectively. The symbols ||. || denote the Euclidean norm, k is the sampling instant, Γ and Λ are diagonal weight matrices, r is the desired output trajectory, and $\Delta U(t_k) = [\Delta u(t_k)...\Delta u(t_{k+M-1})]^T$ is a vector of M future changes of the manipulated variable vector u that are to be determined by the on-line optimization. The control horizon (M) and the prediction horizon (P) are used to adjust the speed of the response and hence to stabilize the feedback behavior. Γ is usually used for tradeoffs between different controlled outputs. Λ, on the other hand, is used to penalize different inputs and thus to stabilize the feedback response.

A disturbance estimate should also be added to y in eq 7, or alternatively it can be absorbed in $r(t_{k+1})$. In the standard MPC implementation, the disturbance is assumed constant over the prediction horizon and is set equal to the difference between plant and model outputs at the present time k. The function of the "additive" constant disturbance in the model prediction is to introduce integral action and thus remove steady-state offset in the presence of model uncertainty or unmeasured disturbances. The usual implementation of MPC involves numerical integration of the model state equations over the prediction horizon P to obtain the future output behavior. Then, the objective function (eq 7) is solved on-line to determine the optimum value of $\Delta U(k)$. Only the current value of Δu, which is the first element of $\Delta U(k)$, is implemented on the plant. At the next sampling instant, the whole procedure is repeated.

4.4. Open-Loop Simulations. Effect of Changes in Wall Temperature. To demonstrate the nonlinearity and instability of the reactor, we simulate the process for step change in the wall temperature (T_w) of magnitude ±0.6 °C (equivalent to ±0.002 dimensionless). The results of the open-loop simulations are shown in Figure 5. As shown by this figure, even for small changes in the wall temperature, the reactor temperature (X_3) and consequently the monomer concentration (X_1) diverge away from the desired steady state. When the wall temperature increases, the heat loss to the surroundings decreases, leading to an increase in the reactor temperature. Because of internal instability, the reactor temperature keeps growing till it reaches another stable steady-state point. The opposite trend is true when the wall temperature decreases. Although higher reactor temperature indicates higher monomer conversion, it occurs at a temperature much larger than the polymer softening temperature. Therefore, in the above two cases, the reactor behavior is unacceptable, and thus a controller is needed to stabilize the process.

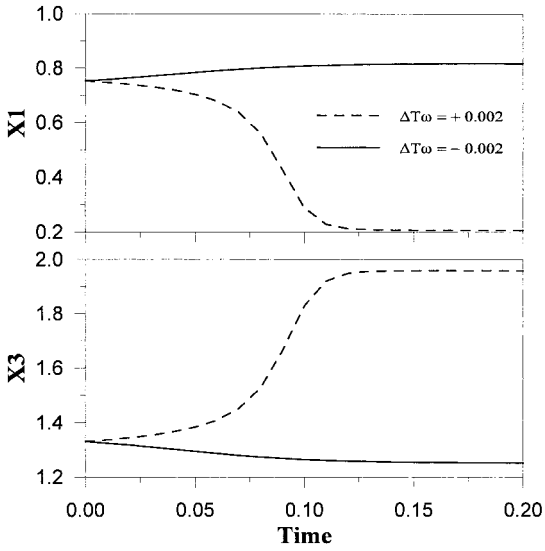

Figure 5. Open-loop simulation for step changes in ΔT_w.

4.5. Closed-Loop Simulations. (i) Disturbance Rejection Using PI Controller. First a single-loop controller, where the feed temperature (T_f) was used as the manipulated variable and the reactor temperature as the controlled variable, will be examined. Usually, T_f is used to stabilize the unstable temperature of fluidized bed reactors.[6,18,19] Dadebo et al.[6] have alternatively used the coolant temperature of an external heat exchanger directly as the manipulated variable. The process closed-loop response to different values of step changes in T_w using the PI controller with T_f as the manipulated variable is shown in Figures 6 and 7. The controller settings are listed in Table 7. The wall temperature was constrained between 300 and 360 K to ensure normal practical reactor operation. Good control performance was observed for a very small perturbation in ΔT_w (Figure 6). However, as indicated by Figure 7, for changes in T_w as low as 6 °C, the feed temperature saturates and reactor ignition occurs, leading to poor performance. Moreover, although the controller was tuned initially using Ziegler and Nichols

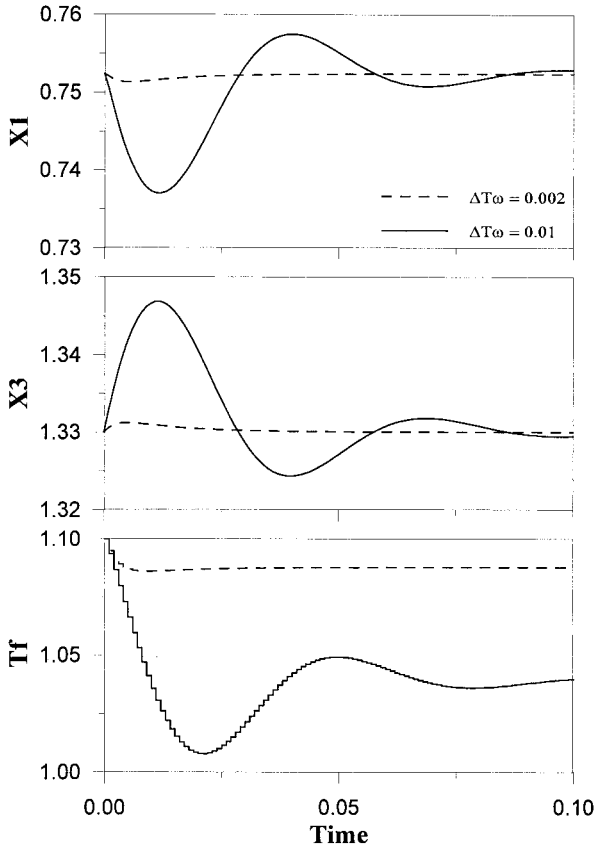

Figure 6. Disturbance rejection response using a PI controller with T_f as the manipulated variable for $\Delta T_w = 0.002$ and 0.01.

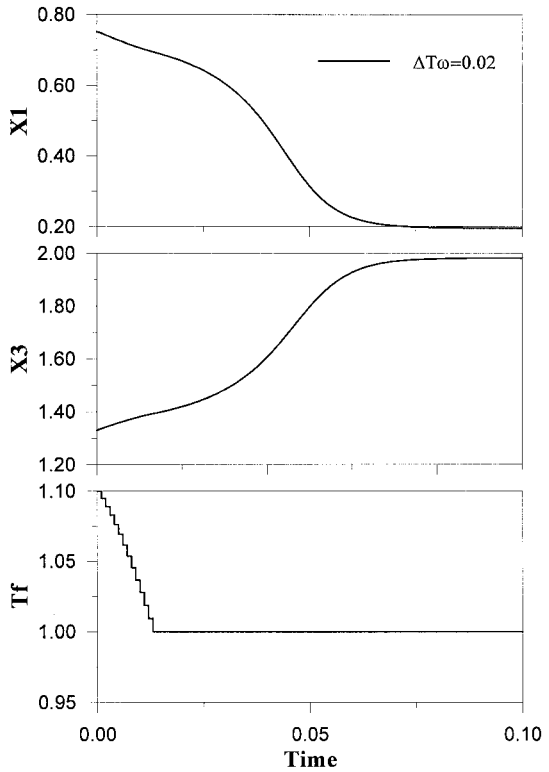

Figure 7. Disturbance rejection response using a PI controller with T_f as the manipulated variable for $\Delta T_w = 0.02$.

method[12] for $\Delta T_w = 0.002$, it had to be retuned for stability for each different value of ΔT_w as listed in Table 7.

Table 7. PI Controller Parameters for $X_3 \rightarrow T_f$ Scheme

case	K_c	τ_I
$\Delta T_w = 0.002$	6000	0.02
$\Delta T_w = 0.01$	1500	0.01
$\Delta T_w = 0.02$	600	0.01

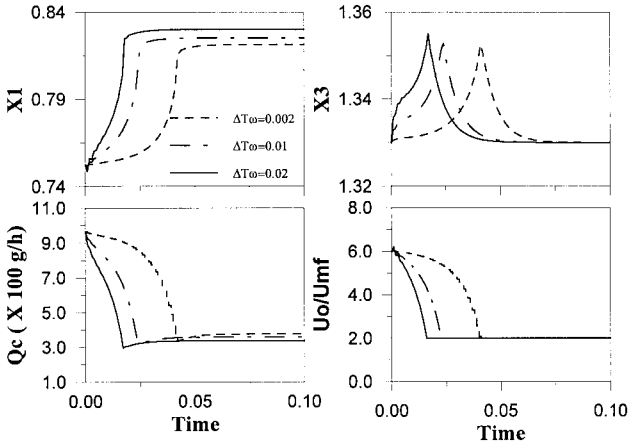

Figure 8. Disturbance rejection response using a PI controller with Q_c and ϕ as the manipulated variables for three values of ΔT_w.

Table 8. PI Controller Parameters for S_1

scheme	K_c	τ_I
$X_1 \rightarrow \phi$	120	0.01
$X_3 \rightarrow Q_c$	300	0.01

To improve the closed-loop performance, a multiloop control scheme should be used. Specifically, the reactor temperature and the monomer concentration should be controlled by any combination of the available three manipulated variables. Figure 8 illustrates the closed-loop response for the same step changes in ΔT_w using Q_c and ϕ (control structure S1) as control variables, as suggested by the NRGA and SVD methods discussed earlier. The controller settings are listed in Table 8. These controller settings were obtained by tuning each loop separately using the Ziegler−Nichols method.[12] Surprisingly, the controller performance was poor, since it could not maintain the first controlled variable at its set point. The performance is also unacceptable from the operation point of view, since the conversion is substantially reduced. This poor performance is attributed to the dangerous interaction effect due to the negative elements of the RGA.[16] Even when the order of input−output pairing was reversed, an unacceptable feedback response was still observed.

For the sake of better closed-loop performance, we tried implementing a different control structure. In this case control structure S2 was selected. Control structure S3 was intentionally avoided because Q_c is already operating in the neighborhood of its upper limit. Improved closed-loop performance was obtained as shown by Figure 9 when the control structure (S2) was used with opposite input−output pairing to the one suggested by the RGA. The controller parameters are listed in Table 9. The proposed input−output pairing recommended by RGA was also tested for the same control problem. However, the controller was unable to stabilize the reactor operation in this case. The simulation results for this case are omitted for brevity.

(ii) Disturbance Rejection Using NLMPC. The performance of the proposed NLMPC for the same regulatory problem investigated above was also exam-

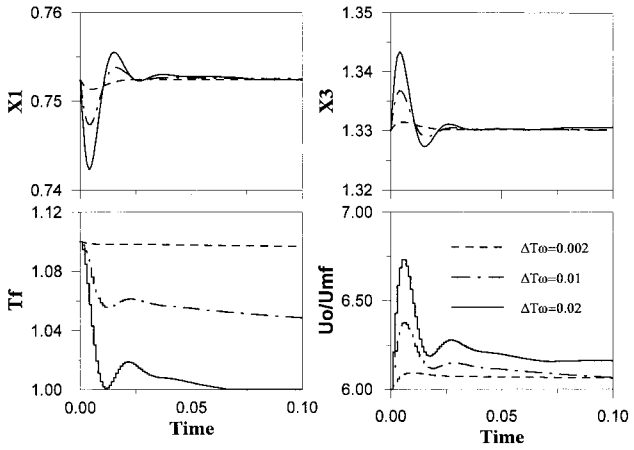

Figure 9. Disturbance rejection response using a PI controller with T_f and ϕ as the manipulated variables for three values of ΔT_w.

Table 9. PI Controller Parameters for S_2

scheme	K_c	τ_I
$X_1 \rightarrow \phi$	120	0.01
$X_3 \rightarrow T_f$	500	0.001

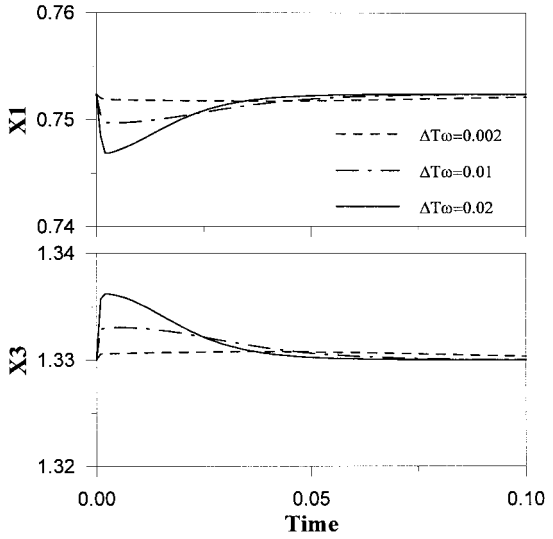

Figure 10. Disturbance rejection response using NLMPC for three values of ΔT_w.

Table 10. NLMC Tuning Parameters

M	P	Λ	Γ
1	1	diag[0,0,0]	diag[1,1]

ined. Since MPC is a multivariable control scheme that allows nonsquare control structure, we will use the three available manipulated variables directly to control X_1 and X_3. The results of the closed-loop simulation are depicted by Figure 10, and the tuning parameter values used are listed in Table 10. The corresponding response of the manipulated variables is shown in Figure 11. It is obvious from the plots that excellent disturbance rejection was obtained. When compared to the closed-loop performance obtained by the PI controller, the feedback response obtained by NLMPC had higher overshoot in X_3 and less overshoot in X_1. However, similar performance can be obtained if Γ is properly adjusted, that is, γ_2 is increased.

Nevertheless, NLMPC out performed the PI in many aspects. First, in the PI case, the control structure

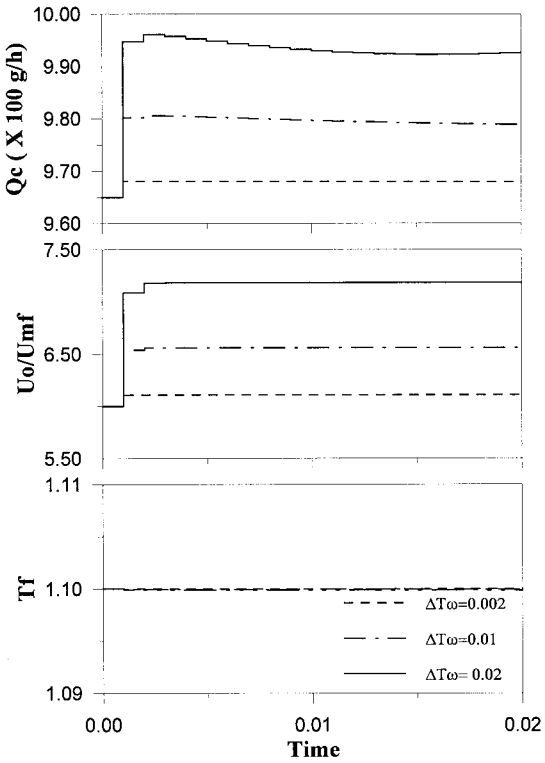

Figure 11. Manipulated variable response for the disturbance rejection in Figure 10.

should be carefully selected as the recommended structure by NRGA and SVD performed inadequately. Second, the PI demanded successive tuning not only for good performance but also for stability. Furthermore, as illustrated by Figure 11, NLMPC has only utilized Q_c and ϕ to stabilize the process, whereas the PI performed poorly using the same pair of manipulated variables. This is because PI treated the two loops as decoupled, which is not completely true. Last, with the 3×2 structure of NLMPC and knowing that none of the manipulated variables had saturated (Figure 11) whereas the feed temperature has already saturated in the PI case (Figure 9), NLMPC has more degrees of freedom and power to reject more excessive disturbances than PI.

(iii) Set Point Tracking Using NLMPC. Instead of simply testing the NLMPC algorithm for any set point tracking, we try to simulate the feedback system to some operating points that are related to the optimal operation of the reactor. In this case, two set point change simulations are considered. First, we tried to operate the reactor temperature at a safe temperature, that is, less than the polymer softening temperature, while maintaining maximum yield. The closed-loop simulation is depicted by Figures 12c and d. The corresponding response of the manipulated variables is shown in Figure 13 by the dash-and-dot lines. The same tuning parameters in Table 10 are used here. The strong interaction is very clear, as shown by the figures. As the controller pushes the reactor temperature to the new set point, the monomer concentration departs away from its desired target. Since equal weights (Γ = diag[1,1]) were used for both outputs, the controller ends with a trade-off. Of course, X_3 can be brought to its new set point by increasing its corresponding weight (γ_2). However, this would be at the expense of monomer conversion.

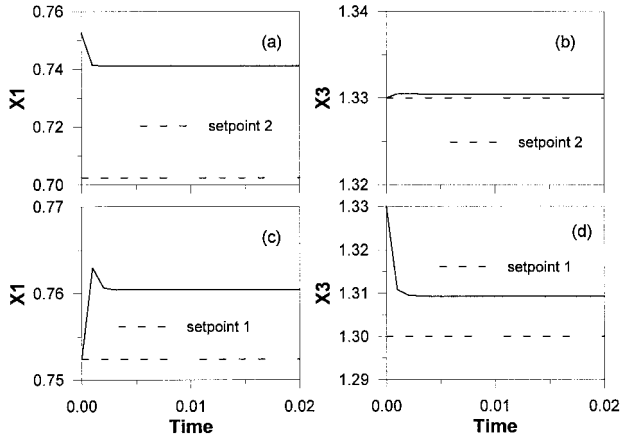

Figure 12. Set point change response using NLMPC: (a and b) set point = [−0.05, 0]; (c and d) set point = [0, −0.03].

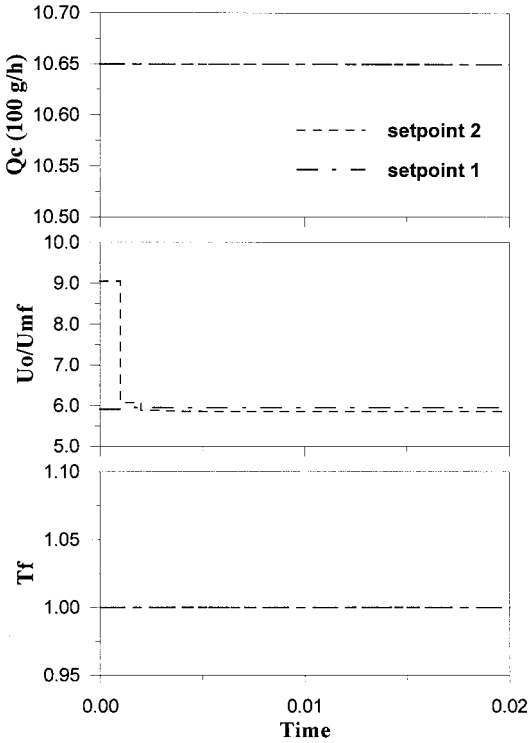

Figure 13. Manipulated variable response for the set point changes in Figure 12.

The second test is to operate the reactor at higher conversion while keeping the reactor temperature at its old steady-state value. The closed-loop response using the tuning parameters in Table 10 but with $\gamma_2 = 10$ is shown in Figures 12a and b, and the corresponding response of the manipulated variables is shown in Figure 13 by the dotted lines. Obviously, with large weight on X_3, since it is more important, higher conversion was not reachable. Moreover, in both tests, the catalyst feed and the feed temperature stuck at their upper and lower bounds, respectively. Thus, these new operating points are not only unachievable but may also cause poor regulatory performance because the inputs saturate, leaving no more room to move to counteract any disturbances.

5. Conclusions

A dynamic model describing an ethylene gas-phase polymerization reaction in a fluidized bed reactor is used here for optimal operation and control of the process. The open-loop bifurcation analysis revealed that the unit was operated in the low-monomer-conversion region (about 5%) due to a polymer-softening temperature limitation. It has also been found that the catalyst feed rate, the gas superficial velocity, and the feed temperature have significant effects on the single-pass monomer conversion. Due to the limitation imposed by the polymer-softening temperature, the maximum attainable conversion is found to be around 25% (20% above the normal operating conversion). However, this optimal operating point which dictates the maximum catalyst feed rate is internally unstable. For this reason and knowing that the reactor temperature must be tightly kept less than or close to the polymer softening temperature, proportional integral (PI) and nonlinear model predictive control (NLMPC) algorithms were employed to control and stabilize the reactor around the desired optimal operating conditions.

The closed-loop simulations using a PI controller revealed that a single control loop with the feed temperature as the manipulated variable is not sufficient to stabilize the reactor temperature against external disturbances. In fact, it has been found that a mutliloop control scheme must be used to improve the feedback response. Interestingly, the control structure recommended by the standard approaches for multiloop control design failed in providing good regulatory performance. Instead, an arbitrary selected control structure was found to be more effective in rejecting the disturbance effect and hence stabilizing the reactor. Another encountered drawback of the PI controller is the necessity to retune the controller parameters from case to case.

On the other hand, the NLMPC out-performed the conventional PI controller. In addition to its excellent closed-loop response, NLMPC was easy to implement. In fact, NLMPC does not require the selection of proper control structure or demand repeated tuning of its parameters. Moreover, simulations revealed that NLMPC, due to its multivariable nature and optimal behavior, had more degrees of freedom and a wider input range than PI to control the process. NLMPC was also employed to find if the process can be brought to more desirable operating conditions such as higher conversions and/or lower reactor temperatures. The first specification was unattained because it requires the reactor temperature to rise much above the polymer melting point. Similarly, the second specification was unacceptable, since it lowers monomer conversion.

Nomenclature

A = cross-sectional area of fluidized bed (cm^2)
A_b = area of bubble phase (cm^2)
B = constant matrix for the linear constraints
b = vector of bounds for the linear constraints
C_0 = inlet monomer concentration (g/cm^3)
k = sampling instant
M = control horizon
Q_c = catalyst injection rate (g/h)
P = prediction horizon
r = set point
S_i = control structure i
T_f = feed temperature (K)
t_k = sampling time
T_w = wall temperature (K)
U_b = bubble velocity (cm/s)

U_0 = inlet gas velocity (cm/s)
U_{mf} = minimum fluidization velocity (cm/s)
X_1, X_2 = dimensionless monomer and catalyst concentration in the dense phase
X_3 = dimensionless dense-phase temperature
x = vector of state variables
Y_0 = dimensionless feed temperature
Y_w = dimensionless wall temperature
y = vector of outputs

Greek Letters

α_i, γ_i = parameters used to nondimensionalize the model equations
Δu = vector of manipulated variables
ΔU = vector of M future manipulated variables
Γ = diagonal weight matrix on outputs
Λ = diagonal weight matrix on inputs
τ = dimensionless time

Abbreviations

HB = Hopf bifurcation point
SPB = stable periodic branch
SSB = stable static branch
UPB = unstable periodic branch
USB = unstable periodic branch

Literature Cited

(1) Meziou, A.; Deshpande, P.; Cozewith, C.; Silverman, C.; Morrison, W. Dynamic Matrix Control of an Ethylene-Propylene-Diene Polymerization Reactor. *Ind. Eng. Chem. Res.* **1996**, *35*, 64.

(2) Choi, K.; Ray, W. The Dynamic Behavior of Fluidized Bed Reactors for Solid Catalyzed Gas-Phase Olefin Polymerization. *Chem. Eng. Sci.* **1985**, *41*, 2261.

(3) Berber, R.; Coskun, S. Dynamic Simulation and Quadratic Dynamic Matrix Control of An Industrial Low-Density Polyethylene Reactor. *Comput. Chem. Eng.* **1996**, *20*, S799.

(4) Lines, B.; Hartien, D.; Paquin, F.; Teiber, S.; deTremblay, M.; Bell, M. Polyethylene Reactor Modeling and Control Design. *Hydrocarbon Process.* **1993**, *6*, 19.

(5) McAuley, K.; McGregor, J. Nonlinear Product Quality Control in Industrial Gas-phase Polyethylene Reactor. *AIChE J.* **1993**, *39*, 855.

(6) Dadebo, S.; Bell, M.; Mclellan, P.; McAuley, K. Temperature Control of Industrial Gas-Phase Polyethylene Reactors. *J. Process Control* **1997**, *7*, 83.

(7) McAuley, K.; Mcgregor, J. Optimal Grade Transitions in a Gas-Phase Polyethylene Reactor. *AIChE* **1992**, *38*, 564.

(8) Xie, T.; McAuely, K.; Hsu, J.; Bacon, D. Gas-Phase Ethylene Polymerization: Production Processes, Polymer Properties, and Reactor Modeling. *Ind. Eng. Chem. Res.* **1994**, *33*, 449.

(9) Wagner, B. E.; Gocke, G. L.; Karol, F. J. Process for the preparation of high-density polymers in fluidized bed reactors. U.S. Patent 4303771, 1981.

(10) Burdett, I. D. The Union Carbide UNIPOL process: Polymerization of olefins in a gas-phase fluidized bed. AIChE annual meeting, Washington, DC, Nov. 27−Dec. 2, 1988.

(11) Abasaeed, A. E.; Al-Zaharni, S. M. Modeling of Fluidized Bed Reactors for the Polymerization Reaction of Ethylene and Propylene. *Dev. Chem. Eng. Mineral Process.* **1998**, *6*, 121.

(12) Ziegler, J. G.; Nichols, N. B. Optimum Settings for Automatic Controllers. *Trans. ASME* **1942**, *64*, 759.

(13) Chang, J.; Yu, C. The Relative Gain for non-square Multivariable Systems. *Chem. Eng. Sci.* **1990**, *45*, 1309.

(14) Cao, Y.; Rossiter, D. An input Pre-screening Technique for control Structure Selection. *Comput. Chem. Eng.* **1997**, *21*, 563.

(15) Cao, Y.; Biss, D. An Extension of Singular Value Decomposition for Assessing Manipulated Variable Constraints. *J. Process Control* **1996**, *6*, 36.

(16) Stephanopoulos, G. *Chemical process control: An Introduction to Theory and Practice*; Prentice-Hall: Englewood Cliffs, NJ, 1984.

(17) Ali, E.; Zafiriou, E. Optimization-Based tuning of Model Predictive Control with State Estimation. *J. Process Control* **1993**, *3*, 97.

(18) Ali, E.; Elnashaie, S. S. Nonlinear Model Predictive Control of Industrial Type IV Fluid Catalytic Cracking (FCC) Units for Maximum Yield. *Ind. Eng. Chem. Res.* **1997**, *36*, 389.

(19) Ali, E.; Ajbar, A. Dynamic Modeling and Control of a Fluidized Bed Reactor for the Oxidative Dehydrogenation of Ethylbenzene to Styrene. *JKSU, Eng. Sci.*, in press.

Received for review January 27, 1998
Revised manuscript received May 1, 1998
Accepted May 4, 1998

IE980048+